Synthesis and Properties of New Mixed-Halide Derivatives of Iron-Sulfide Dimers – Crystal Structure of $(Et_4N)_2[Fe_2S_2Cl_2Br_2]$

Corinne Tonon*[a], Hélène Ierno[a], Jean Laugier[b], Jean-Marc Grenèche[c], and Jeanne Jordanov*[a]

CEA, Département de Recherche Fondamentale sur la Matière Condensée/SCIB/SCPM[a], F-38054 Grenoble cedex 9, France

CEA, Département de Recherche Fondamentale sur la Matère Condensée/Groupe Structures[b], F-38054 Grenoble cedex 9, France

Faculté des Sciences, Laboratoire de Physique de l'Etat Condensé (URA CNRS 807)[c], F-72017 Le Mans cedex, France

Received July 8, 1996

Keywords: Iron-sulfur cluster / Mixed halide ligands / Magnetic properties / Clusters / Iron compounds / Sulfur compounds / Halogen compounds

The synthesis and characterization of the new mixed-halide clusters $(Et_4N)_2[Fe_2S_2Cl_{4-n}Br_n]$ (n = 2, 3), together with an improved synthesis of $(Et_4N)_2[Fe_2S_2Br_4]$ and the crystal and molecular structure of $(Et_4N)_2[Fe_2S_2Cl_2Br_2]$, are reported here. The structure consists of $[Fe_2S_2Cl_2Br_2]$ dianions, with a pseudo-tetrahedral symmetry around each iron atom. A disorder problem precludes precise identification of the locations of the chloride and bromide ligands. A *syn* (or *anti*) conformation is however considered to be most likely, for steric hindrance reasons and on the basis of Mössbauer data. The Mössbauer, magnetic susceptibility, cyclic voltammetry and UV/Vis properties of the new clusters remain similar to those of the parent single-type halide clusters. These new clusters are interesting precursors for complexes with mixed thiolate and non-thiolate coordination at the iron sites.

Introduction

Numerous iron-sulfur clusters with terminal halide ligands have been reported since 1977. These include the $[Fe_2S_2X_4]^{2-}$ (X = Cl, Br, I) series[1–4], and the related tetranuclear $[Fe_4S_4X_4]^{2-}$ dianions[1,2,4–6]. Additional members of the iron/sulfur/halide series are $[Fe_6S_6X_6]^{2-/3-}$ (X = Cl, Br, I) clusters[5,7–10]. Most of these Fe/S/X clusters have been used as starting compounds for further substitution of the halides by other ligands. Thus, $[Fe_2S_2Cl_4]^{2-}$ and $[Fe_4S_4Cl_4]^{2-}$ have been extensively used in ligand-exchange reactions[11–17]. Iron/sulfur/halide clusters have also been used for the synthesis of [2Fe–2S] and [4Fe–4S] clusters with *mixed* terminal ligands, by partial and/or stepwise substitution of the halides. Indeed, mixed-ligand clusters may be considered as models for a newly emerging structural class of iron-sulfur proteins, where a partly noncysteine coordination is reponsible for site-differentiated Fe–S clusters (e.g. Rieske protein[18], *P. furiosus* ferredoxin[19], *D. africanus* ferredoxin III[20], and *D. gigas* hydrogenase[21]). Mixed-ligand clusters obtained thus far comprise $[Fe_4S_4Cl_3(Et_2dtc)]^{2-}$[22], $[Fe_4S_4X_2(L)_m]^{n-}$ (L = OPh, SPh, Et_2dtc, X = Cl, $m = n = 2$; L = $SPPh_3$, X = I; $m = 2$, $n = 0$; L = *t*-BuNC, X = Cl, $m = 6$, $n = 0$)[22–25], as well as the series $[Fe_2S_2(L–L')_2]^{2-}$, where L–L' are bidentate bis (phenolate)[26] or mixed benzimidazolate-thiolate, -phenolate and bis(benzimidazolate) terminal ligands[27,28]. However, these clusters are often isolated from equilibrium or statistical mixtures, which precludes generalization of this method. It may therefore be of interest to synthesize iron-sulfur clusters with labile terminal ligands that differ somewhat in their leaving abilities, as precursors for complexes with mixed thiolate *and* non-thiolate coordination at the iron sites.

We recently became interested in the obtention of iron-sulfur clusters with a mixed thiolate/imidazole coordination as models for the [2Fe–2S] Rieske centre, and therefore had to devise suitable starting clusters. We describe here the synthesis and characterization of the new mixed-halide complexes $[Fe_2S_2Cl_{4-n}Br_n]^{2-}$ (n = 2, 3), together with the crystal and molecular structure of $(Et_4N)_2[Fe_2S_2Cl_2Br_2]$. Also reported is an improved synthesis of $(Et_4N)_2[Fe_2S_2Br_4]$.

Results and Discussion

Synthesis of Clusters

The (mixed) halide clusters (with m = 1, n = 2; m = 2, n = 3; m = 3 or 4, n = 4) are prepared in good yields following reaction 1:

Scheme 1

$$2\,(Et_4N)(FeCl_{4-m}Br_m) + 2\,(Me_3Si)_2S \longrightarrow (Et_4N)_2[Fe_2S_2Cl_{4-n}Br_n] + (4-2m+n)Me_3SiCl + (2m-n)Me_3SiBr \quad (1)$$

$m=0$	$2\,[FeCl_4]^-$	$-4\,Cl^-$	$[Fe_2S_2Cl_4]^{2-}$	$n=0$
$m=1$	$2\,[FeCl_3Br]^-$	$-4\,Cl^-$		
$m=2$	$2\,[FeCl_2Br_2]^-$	$-3\,Cl^-$, $-Br^-$	$[Fe_2S_2Cl_2Br_2]^{2-}$	$n=2$
$m=3$	$2\,[FeClBr_3]^-$	$-2Cl^-$, $-2\,Br^-$	$[Fe_2S_2ClBr_3]^{2-}$	$n=3$
$m=4$	$2\,[FeBr_4]^-$	$-4\,Br^-$	$[Fe_2S_2Br_4]^{2-}$	$n=4$

[+] Present address: Manufacture Michelin, F-63040 Clermont-Ferand Cedex 1, France.

  0009–2940/97/0202–0235 $ 15.00+.25/0

This procedure had previously been reported only for the all-chloride derivative ($m = n = 0$)[3], and has been extended here to the mixed chloride/bromide derivatives. In the case of $[Fe_2S_2Br_4]^{2-}$, the above reaction is an improvement over an earlier two-step method, as it avoids preparation of the intermediate $(R_4N)_2[Fe_2S_2(S_2\text{-}o\text{-xylyl})_2]$.

The halide stoichiometries of the final compounds do not appear to be ruled by a statistical distribution of the leaving chlorides and bromides. Indeed, if that were the case, reaction 1 with $[FeCl_3Br]^-$ should give 25% $[Fe_2S_2Cl_4]^{2-}$, 50% $[Fe_2S_2Cl_3Br]^{2-}$ and 25% $[Fe_2S_2Cl_2Br_2]^{2-}$, and this would be in contradiction both with the elemental analysis and the 81% yield actually obtained for the isolated product (on the other hand, one cannot exclude that when the final compounds are left in solution, they may undergo statistical redistribution). The chloride is known to be a better nucleophile than the bromide in the Si–S bond-cleavage reaction and in the subsequent formation of $(CH_3)_3SiX$. The chlorides are thus likely to be the preferred leaving groups. The bromides will also become leaving groups when more than one bromide per iron is present, possibly for steric hindrance reasons. The substitution reaction is then slowed down, as indicated by the observation that $[Fe_2S_2ClBr_3]^{2-}$ and $[Fe_2S_2Br_4]^{2-}$ crystallize more slowly out of solution.

X-ray Structural Analysis of $(Et_4N)_2[Fe_2S_2Cl_2Br_2]$

Two $[Fe_2S_2Cl_2Br_2]$ dianions are located on symmetry centers in the unit cell, and the asymmetric unit contains one FeSClBr moiety and one Et_4N cation. Initially a Fourier synthesis showed that if the Fe peak density is normalized to 26, then the peak density of the two neighboring sites is approximately 20, which is intermediate between 17 (Cl) and 35 (Br). This indicated a disorder problem, most probably due to the fact that each of these two sites is occupied by a Br + Cl mixture. A first type of refinement was carried out by assuming that each site is occupied by an average atom (Br for instance) and refining its population. From the Br deficit (or Cl excess), the Br and Cl percentages at each site were deduced (this procedure assumes that the form factors for both types of atoms are homothetical, which is true only to a first approximation). A different refinement was therefore then performed: a $Cl_x + Br_{1-x}$ mixture was assumed at each site, and occupancies for both atoms were allowed to vary (the same isotropic thermal coefficient for both atoms was considered). This led to 0.52 Cl + 0.48 Br at site 1, and 0.70 Cl + 0.30 Br at site 2. Then, the percentages of the respective halides were kept fixed and the atomic positions and the anisotropic thermal coefficients were refined. An ORTEP representation of the dianion and one cation is shown in Figure 1. The present structure determination indicates a random distribution of the chlorides and the bromides, and also an excess of chloride vs. bromide: the Cl/Br ratio is approximately 1.6 instead of 1. Elemental analysis for Br and Cl was therefore performed on the same batch from which the crystal used for the X-ray determination had been selected. The analysis confirmed this Cl excess in the crystals, with a Cl/Br ratio of approximately 1.5 instead of 1, as in the initial microcrystalline powder. This implies that the single crystals of $(Et_4N)_2[Fe_2S_2Cl_2Br_2]$ also contain approximately 25% of $(Et_4N)_2[Fe_2S_2Cl_4]$ {or of $(Et_4N)_2[Fe_2S_2Cl_3Br]$}, thereby indicating that some halide dissociation and redistribution does occur, but only when $(Et_4N)_2[Fe_2S_2Cl_2Br_2]$ is left in solution for an extended length of time. On the other hand, the X-ray powder diffraction pattern of the ground crystals is different from that of either $(Et_4N)_2[Fe_2S_2Cl_4]$ or $(Et_4N)_2[Fe_2S_2Br_4]$, or their mixture. This is a clear indication that $(Et_4N)_2[Fe_2S_2Cl_2Br_2]$ cannot be considered as a cocrystallization product of these two parent compounds.

Figure 1. ORTEP diagram showing the structure and atom labeling for $(Et_4N)_2[Fe_2S_2Cl_2Br_2]$ (the thermal ellipsoids are drawn at 50% probability level). Selected bond lengths (Å) and angles (°): Fe–Cl(1) 2.30(1), Fe–Cl(2) 2.31(1), Fe–Br(1) 2.370(7), Fe–Br(2) 2.32(1), Fe–S 2.197(2), Fe–Fe 2.711(1); Fe–S–Fe 76.2(0), S–Fe–S 103.8(0), Br(1)–Fe–Br(2) 102.7(5), Cl(1)–Fe–Cl(2) 112.2(6), Br(1)–Fe–Cl(2) 105.9(5), Br(2)–Fe–Cl(1) 108.9(6), Br(1)–Fe–S 112.3(2), Br(2)–Fe–S 113.0(4), Cl(1)–Fe–S 109.0(3), Cl(2)–Fe–S 111.1(4)

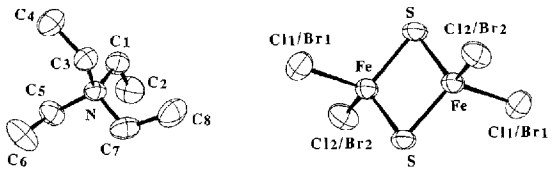

Both distances and angles of the Fe_2S_2 core are very similar (within experimental error) to those previously determined in $[Fe_2S_2Cl_4]^{2-}$[1]. In contrast, the Fe–Cl distances (2.304 and 2.316 Å) are somewhat longer than in the all-chloride dianion, and the Fe–Br distances (2.321 and 2.370 Å) are quite unequal. The latter values are comparable to the Fe–Br distances determined in $(Ph_4P)_2[Fe_4S_4Br_4]$[4], where they range from 2.338 to 2.345 Å.

This disorder problem most probably arises from the fact that some $(Et_4N)_2[Fe_2S_2Cl_4]$ cocrystallizes together with $(Et_4N)_2[Fe_2S_2Cl_2Br_2]$, but also from the probable coexistence within the crystal of the *anti*, *syn* and dissymetric conformers of $[Fe_2S_2Cl_2Br_2]^{2-}$ (Scheme 2). A similar problem was recently reported by Wieghardt and coworkers[33] for the $[Fe_2Cl_6O]^{2-}$ dianion.

Scheme 2. Possible conformations of the $[Fe_2S_2Cl_2Br_2]^{2-}$ anion in crystals of $(Et_4N)_2[Fe_2S_2Cl_2Br_2]$

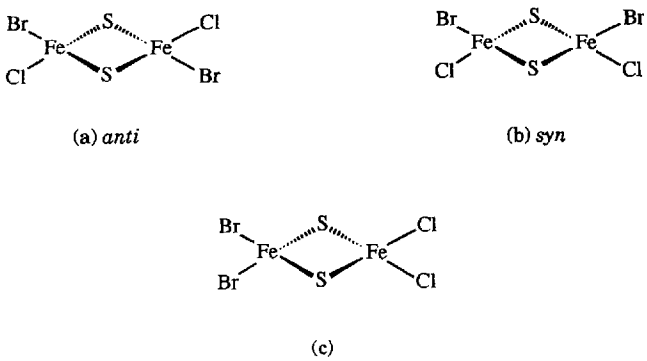

Mössbauer Spectroscopy and Magnetic Susceptibility Data

The parameters obtained from the least-squares fitting of the Mössbauer spectra for the NEt_4 salts of $[Fe_2S_2Cl_4]^{2-}$, $[Fe_2S_2Cl_2Br_2]^{2-}$ and $[Fe_2S_2Br_4]^{2-}$ are listed in Table 1. The spectra are characterized by single quadrupole-split doublets, with isomer shift δ and quadrupole splitting ΔE_Q parameters that identify them as high-spin ferric clusters. The linewidths remain quite narrow (0.27–0.28 mm s^{-1}) and similar to those generally found in iron-sulfur clusters, and are indicative of the homogeneity of the iron sites. In the case of $(Et_4N)_2[Fe_2S_2Cl_2Br_2]$, the spectrum was run on a sample of ground crystals, and was best fitted with two subcomponents. Site I (which accounts for approximately 75% of the total iron present) was assigned to the principal species $(Et_4N)_2[Fe_2S_2Cl_2Br_2]$, as its quadrupole splitting value is different from both that of $(Et_4N)_2[Fe_2S_2Cl_4]$ and $(Et_4N)_2[Fe_2S_2Br_4]$. Site II contributes approximately 20% of the overall spectrum, and its parameters are consistent with those of $(Et_4N)_2[Fe_2S_2Cl_4]$ (δ = 0.36 mm s^{-1}, ΔE_Q = 0.78 mm s^{-1}), which has already been shown to cocrystallize as a minority species (see above). The difference in the isomer shift values compared to those of other Fe_2S_2 clusters is consistent with the fact that halides are less electron donating than thiolate ligands, for which isomer shift values of 0.20–0.30 mm s^{-1} are generally found. The larger isomer shifts observed here are within the range found in the cases of phenolate[11] and *o,o'*-bisphenolate[26] coordination (0.35–0.37 mm s^{-1}). The isomer shift invariance observed when going from the all-chloride to the all-bromide cluster indicates that there is no change in the charge localization. On the other hand, the quadrupole splitting values increase slightly with the bulkiness of the halides and with the decrease of local symmetry at each iron site. Thus $(Et_4N)_2[Fe_2S_2Cl_2Br_2]$ is characterized by the highest value of ΔE_Q = 0.97 mm s^{-1}. This indicates that the iron sites in the latter cluster are in a more distorted environment than in either the $[Fe_2S_2Cl_4]^{2-}$ or $[Fe_2S_2Br_4]^{2-}$ species. This observation is in support of geometry (a) or (b) rather than (c) (Scheme 2) for the $[Fe_2S_2Cl_2Br_2]$ dianion.

The magnetic susceptibilities of the Et_4N^+ salts of $[Fe_2S_2Cl_4]^{2-}$, $[Fe_2S_2Cl_2Br_2]^{2-}$ and $[Fe_2S_2Br_4]^{2-}$ were measured in the temperature range 2–315 K. The observed temperature dependence is indicative of the existence of an antiferromagnetic coupling between the two high-spin ferric ions. The data were least-squares fitted to the theoretical equation for an isotropic magnetic exchange interaction between two spins $S_1 = S_2 = 5/2$[34], by employing the spin Hamiltonian $H = JS_1 \cdot S_2$. The experimental and theoretical plots of $\chi T = f(T)$ are reported in Figure 2, and fitting parameters are listed in Table 1. Because of the presence of a ferromagnetic impurity in $[Fe_2S_2Br_4]^{2-}$, data for it below 50 K were not included during the fitting procedure. In the case of the other two clusters, the fitting involved either the whole temperature range or only the data in the 50–315 K range. This did not affect the J values. Thus, the best-fit values for the antiferromagnetic coupling constants of the Fe^{3+}-Fe^{3+} pairs of the above clusters are 383, 421 and 387 cm^{-1} respectively, which indicates that the antiferromagnetic interaction is nearly independent of the progressive replacement of the chlorides by the bromides. These values are comparable to those determined, using the same Hamiltonian, for oxidized two-Fe ferredoxins (ca. 370 cm^{-1})[35,36]. The antiferromagnetic coupling constant for $[Fe_2S_2Cl_4]^{2-}$ has previously been reported to be 316 cm^{-1}, with however a lack of agreement between experiment and theory below 140 K. This value should therefore be considered as less reliable.

Solution Studies

Solution studies were carried out mainly for characterization purposes. The cyclic voltammetry of the $[Fe_2S_2Cl_{4-n}Br_n]^{2-}$ (n = 2, 3) clusters was studied in CH_3CN solution (Table 1). The mixed-halide clusters exhibit only a cathodic wave, corresponding to formation of the trianions, accompanied by a further reduction in the −1.7/−1.8 V region, which has been associated with the $[Fe_4S_4X_4]^{3-/4-}$ process. This behavior is consistent with dimerization of the chemically unstable trianion $[Fe_2S_2Cl_{4-n}]Br_n]^{3-}$ into $[Fe_4S_4Cl_{4-n}Br_n]^{3-}$, followed by reduction of the latter, as already reported in the case of $[Fe_2S_2X_4]^{2-}$ (X = Cl, Br)[2]. As in the $[Fe_2S_2X_4]^{2-}$, $[Fe_4S_4X_4]^{2-}$ and $[Fe_6S_6X_6]^{2-}$ (X = Cl, Br, I) series[2,7], the reduction potentials become less

Table 1. Selected Mössbauer, magnetic, electronic absorption data and redox potentials for $(Et_4N)_2[Fe_2S_2Cl_{4-n}Br_n]$ (n = 0, 2, 3, 4)

Compound	δ / ΔE_Q / Γ[b,c], mm/s	J, Hz (p)[d]	E_{pc}, V	λ_{max}, nm (ε_M, $M^{-1}cm^{-1}$)
$(Et_4N)_2[Fe_2S_2Cl_4]$[a]	0.37 / 0.81 / 0.27	383 (0.01)	−98	358, 406, 456, 520, 572
$(Et_4N)_2[Fe_2S_2Cl_2Br_2]$	(I) 0.36 / 0.97 / 0.28	421 (0.002)	−90	360 (4524), 408 (1913)
	(II) 0.36 / 0.78 / 0.28			464 (2933), 522 (1918)
				580 (1647)
$(Et_4N)_2[Fe_2S_2ClBr_3]$			−88	368, 416, 472, 590
$(Et_4N)_2[Fe_2S_2Br_4]$[a]	0.36 / 0.91 / 0.27	387 (0.08)	−80	370, 418, 478, 596

[a] Our data for E_{pc} and λ_{max} are in good agreement with those reported in ref. 2. – [b] Linewidths Γ are expressed as the full width at half maximum. – [c] Errors are estimated to be ±1% on the Mössbauer parameters, ±10 cm^{-1} on the J values. – [d] The g value was kept fixed at 2.0 during the fitting procedure; p is a variable paramagnetic (S = 5/2) impurity.

Figure 2. Plots of $\chi \cdot T$ versus temperature for $(Et_4N)_2[Fe_2S_2Cl_4]$, $(Et_4N)_2[Fe_2S_2Cl_2Br_2]$ and $(Et_4N)_2[Fe_2S_2Cl_4]$ (solid lines represent least-squares best fits to experimental data)

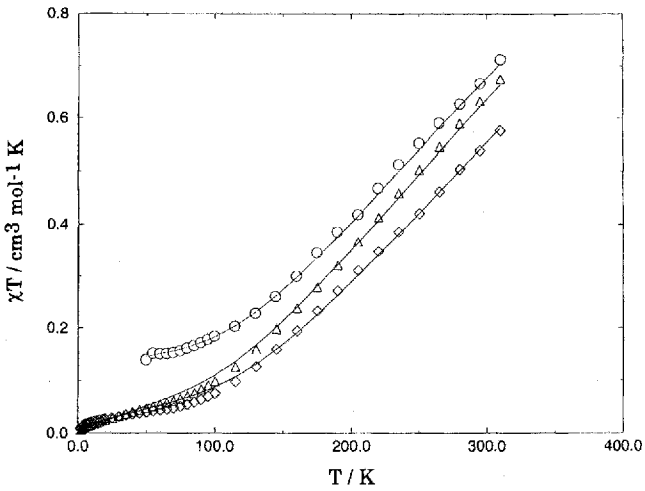

negative when increasing the overall number of bromides (increasing n), following the decreasing electronegativity of the respective halides. The electronic absorption spectra consist of a series of characteristic features (Table 1) that are shifted to progressively lower energies on increasing the number of bromides present in the complexes. A similar ligand-dependent energy shift has been observed in the $[Fe_2S_2X_4]^{2-}$, $[Fe_4S_4X_4]^{2-}$ and $[Fe_6S_6X_6]^{2-}$ (X = Cl, Br, I) series[2,7] as well as in $[Fe_2S_2L_4]^{2-}$ (L = OPh, SPh)[11], and has been attributed to the decreasing electronegativity of the terminal ligands upon the $X \rightarrow Fe_2S_2$ core charge-transfer excitations. We failed to detect any equilibrium components due to a dissociation reaction, but this is probably due to the low resolving abilities of cyclic voltammetry and electronic absorption spectroscopy.

Conclusion

The $[Fe_2S_2Cl_{4-n}Br_n]^{2-}$ (n = 2, 3) species are new members of the general series of iron/sulfur/halide clusters where two different halides are bound to the iron atoms. Their spectroscopic, magnetic and electrochemical properties are very similar to those of the parent single-type halide clusters. From the results of solution studies on the new clusters and previous knowledge of other Fe–S clusters, it is possible that a (slow) statistical redistribution of the halides occurs in solution over all the Fe–S cores, with the resulting coexistence of the various equilibrium components. Indeed, when $(Et_4N)_2[Fe_2S_2Cl_2Br_2]$ is allowed to recrystallize slowly, some $(Et_4N)_2[Fe_2S_2Cl_4]$ is also formed. However, $[Fe_2S_2Cl_2Br_2]^{2-}$ remains the principal component of the resulting single crystals, most likely with one chloride and one bromide per iron, in the *syn* and/or *anti* conformations. The structural homogeneity of these new mixed-halide Fe–S clusters in the solid state is further supported by the Mössbauer parameters, which show single iron sites. We are currently investigating the use of these new clusters as starting compounds for mixed sulfur/nitrogen ligand coordination at the iron sites.

Experimental Section

All reactions were performed in a prepurified argon atmosphere by using standard Schlenk techniques or a Jacomex glovebox. Solvents were dried and distilled under argon before use. Tetraethylammonium salts of $[FeClBr_3]^-$, $[FeCl_2Br_2]^-$, $[FeCl_3Br]^-$ and $[Fe_2S_2Cl_4]^{2-}$ were prepared according to published methods[3,29].

Syntheses: $(Et_4N)_2[Fe_2S_2Cl_2Br_2]$ was synthesized by the same procedure[3] as described for $(Et_4N)_2[Fe_2S_2Cl_4]$, with $(Et_4N)[FeCl_3Br]$ as a starting salt. Yield 81%. – $C_{16}H_{40}N_2Cl_2Br_2S_2Fe_2$: calcd. C 28.79, H 6.00, N 4.20, Cl 10.64, Fe 16.79; found C 29.6, H 6.2, N 4.3, Cl 10.0, Fe 16.7. In the case of $(Et_4N)_2[Fe_2S_2ClBr_3]$ and $(Et_4N)_2[Fe_2S_2Br_4]$[30], the above procedure was somewhat modified (using respectively $(Et_4N)[FeCl_2Br_2]$ and $(Et_4N)[FeClBr_3]$ as starting salts): instead of a reaction time of 0.5 h, the solution containing the starting salt and hexamethyldisilylthiane was stirred for 5 h at room temperature, then stored overnight at −20°C. The resulting microcrystalline solid was washed with THF then diethyl ether, to provide respectively $(Et_4N)_2[Fe_2S_2ClBr_3]$ and $(Et_4N)_2[Fe_2S_2Br_4]$, with yields of 66% and 60%. – $C_{16}H_{40}N_2ClBr_3S_2Fe_2$: calcd. C 26.98, H 5.62, N 3.93, Br 33.73, Fe 15.74; found C 27.1, H 5.6, N 3.8, Br 33.6, Fe 15.0. $(Et_4N)_2[Fe_2S_2Br_4]$ was identified by elemental analyses and by its UV/Vis spectrum.

Crystal Structure Determination and Refinement: Suitable crystals of $(Et_4N)_2[Fe_2S_2Cl_2Br_2]$ were grown from CH_3CN/THF solutions after 10 d. A crystal of approximately 0.3 × 0.3 × 0.3 mm was mounted under argon in a sealed Lindeman capillary, and data were collected with a Nonius CAD4 diffractometer, graphite monochromator, Mo-K_α radiation (λ = 0.71073 Å). Intensities were corrected for Lorentz and polarization effects, but not for absorption. The structure was solved by Patterson synthesis, using the SHELX86 package[31], and completed by Fourier difference maps. Positional and anisotropic thermal parameters for all non-hydrogen atoms were refined by full-matrix least-squares methods with the SHELX76 package[32]. All hydrogen atoms were added at calculated positions, with the geometrical constraint C–H = 1.08 Å[37]. $C_{16}H_{40}N_2Fe_2S_2Cl_2Br_2$ (M = 1334.08 g/mol); monoclinic, space group $P2_1/n$; a = 8.978(3), b = 10.253(3), c = 15.471(4) Å, β = 104.08(1)°, V = 1381.08(1) Å^3, Z = 2; D_{calc} = 1.59 g · cm^{-3}; ω scan; Θ range: 1–30°; 4647 reflections collected; 2194 unique reflections ($F > 4\sigma$); 136 variables refined; $w^{-1} = \sigma^2(F_o) + gF_o^2$, R = 0.036, R_w = 0.030.

Physical Techniques: Cyclic voltammetry was performed using a PAR 273 potentiostat, and a standard three-electrode system, with platinum working and counter electrodes. The Ag/AgCl reference electrode was checked against the ferrocenium/ferrocene couple. The supporting electrolyte was Bu_4NPF_6 (0.1 M). All potentials are given relative to SCE. Electronic absorption spectra were recorded on a HP 8452A diode array spectrophotometer. Magnetic susceptibility data were obtained by use of a Quantum Design SQUID susceptometer. The magnetization measurements were performed at nonsaturating fields (H = 0.5 T), in the 2–315 K temperature range. Mössbauer data were collected at 77 K, on finely ground samples containing 5–10 mg Fe/cm^2 located in plexiglas air-tight capsules, using a conventional constant acceleration spectrometer with a ^{57}Co source diffused in a rhodium matrix maintained at room temperature. Isomer shifts are quoted relative to Fe metal at 300 K. The powder diffraction diagrams were obtained by using a 114-nm diameter Debye-Scherrer-type camera with Ni-filtered Cu-K_α radiation. Elemental analyses were carried out at the Service Central d'Analyses du CNRS in Vernaison, France.

[1] M. A. Bobrik, K. O. Hodgson, R. H. Holm, *Inorg. Chem.* **1977**, *16*, 1851–1858.
[2] G. B. Wong, M. A. Bobrik, R. H. Holm, *Inorg. Chem.* **1978**, *17*, 578–584.
[3] Y. Do, E. D. Simhon, R. H. Holm, *Inorg. Chem.* **1983**, *22*, 3809–3812.
[4] A. Müller, N. H. Schladerbeck, E. Krickemeyer, H. Bögge, K. Schmitz, E. Bill, A. X. Trautwein, *Z. Anorg. Allg. Chem.* **1989**, *570*, 7–36.
[5] W. Saak, S. Pohl, *Z. Naturforsch.* **1985**, *40b*, 1105–1112.
[6] D. Coucouvanis, M. G. Kanatzidis, E. Simhon, N. C. Baenziger, *J. Am. Chem. Soc.* **1982**, **104**, 1874–1882.
[7] M. G. Kanatzidis, W. R. Hagen, W. R. Dunham, R. K. Lester, D. Coucouvanis, *J. Am. Chem. Soc.* **1985**, *107*, 953–961.
[8] M. G. Kanatzidis, A. Salifoglou, D. Coucouvanis, *Inorg. Chem.* **1986**, *25*, 2460–2468.
[9] W. Saak, G. Henkel, S. Pohl, *Angew. Chem. Int. Ed. Engl.* **1984**, *23*, 150–151.
[10] D. Coucouvanis, M. G. Kanatzidis, W. R. Dunham, W. R. Hagen, *J. Am. Chem. Soc.* **1984**, *106*, 7998–7999.
[11] W. E. Cleland, Jr., B. A. Averill, *Inorg. Chem.* **1984**, *23*, 4192–4197.
[12] P. Beardwood, J. F. Gibson, *J. Chem. Soc., Chem. Commun.* **1985**, 102–104.
[13] D. Coucouvanis, A. Salifoglou, M. G. Kanatzidis, A. Simopoulos, V. Papaefthymiou, *J. Am. Chem. Soc.* **1984**, *106*, 6081–6082.
[14] S. Ueno, N. Ueyama, A. Nakamura, T. Tukihara, *Inorg. Chem.* **1986**, *25*, 1000–1005.
[15] N. Ueyama, S. Ueno, T. Sugawara, K. Tatsumi, A. Nakamura, N. Yasuoka, *J. Chem. Soc., Dalton Trans.* **1991**, 2723–2727.
[16] W. E. Cleland, D. A. Holtman, M. Sabat, J. A. Ibers, G. C. De Fotis, B. A. Averill, *J. Am. Chem. Soc.* **1983**, *105*, 6021-6027.
[17] C. F. Martens, H. L. Blonk, T. Bongers, J. G. M. van der Linden, G. Beurskens, P. T. Beurskens, J. M. M. Smits, R. J. M. Nolte, *J. Chem. Soc., Chem. Commun.* **1991**, 1623–1625.
[18] R. J. Gurbiel, C. J. Batie, M. Sivaraja, A. E. True, J. A. Fee, B. M. Hoffman, D. P. Ballou, *Biochemistry* **1989**, *28*, 4861–4871.
[19] R. C. Conover, A. T. Kowal, W. Fu, J. B. Park, S. Aono, M. W. W. Adams, M. K. Johnson, *J. Biol. Chem.* **1990**, *265*, 8533–8541.
[20] S. J. George, F. A. Armstrong, E. C. Hatchikian, A. J. Thomson, *Biochem. J.* **1989**, *264*, 275–284.
[21] A. Volbeda, M. H. Charon, C. Piras, E. C. Hatchikian, M. Frey, J. C. Fontecilla-Camps, *Nature* **1995**, *373*, 580–587.
[22] M. G. Kanatzidis, D. Coucouvanis, A. Simopoulos, A. Kostikas, V. Papaefthymiou, *J. Am. Chem. Soc.* **1985**, *107*, 4925–4935.
[23] M. G. Kanatzidis, N. C. Baenziger, D. Coucouvanis, A. Simopoulos, A. Kostikas, *J. Am. Chem. Soc.* **1984**, *106*, 4500–4511.
[24] W. Saak, S. Pohl, *Z. Naturforsch.* **1988**, *43B*, 813–827.
[25] J. A. Weigel, K. K. P. Srivastava, E. P. Day, E. Münck, R. H. Holm, *J. Am. Chem. Soc.* **1990**, *112*, 8015.
[26] A. Salifoglou, A. Simopoulos, A. Kostikas, R. W. Dunham, M. G. Kanatzidis, D. Coucouvanis, *Inorg. Chem.* **1988**, *27*, 3394.
[27] P. Beardwood, J. F. Gibson, *J. Chem. Soc., Chem. Commun.* **1985**, 1345–1347.
[28] P. Beardwood, J. F. Gibson, *J. Chem. Soc., Chem. Commun.* **1992**, 2457–2466.
[29] C. A. Clausen III, M. L. Good, *Inorg. Chem.* **1970**, *9*, 220–223.
[30] $(Et_4N)_2[Fe_2S_2Br_4]$ could also be prepared by using $(Et_4N)[FeBr_4]$ as a starting salt.
[31] G. M. Sheldrick, "SHELX86 Program for Crystal Structure Solution" University of Göttingen, Germany, 1986.
[32] G. M. Sheldrick, "SHELX76 Program for Crystal Structure Determination" University of Cambridge, U.K., 1976.
[33] G. Haselhorst, K. Wieghardt, S. Keller, B. Schrader, *Inorg. Chem.* **1993**, *32*, 520.
[34] C. O'Connor, *Prog. Inorg. Chem.* **1982**, *29*, 203–283.
[35] G. Palmer, W. R. Dunham, J. A. Fee, R. H. Sands, T. Iizuka, T. Yonetani, *Biochim. Biophys. Acta* **1971**, *245*, 201–207.
[36] L. Petersson, R. Cammack, K. K. Rao, *Biochim. Biophys. Acta* **1980**, *622*, 18–24.
[37] Further details of the crystal structure investigations are available on request from Fachinformationszentrum Karlsruhe, Gesellschaft für wissenschaftlich-technische Information mbH, D-76344 Eggenstein-Leopoldshafen, Germany, on quoting the depository number CSD-406088, the names of the authors and the journal citation.

[96133]